

**SYNTHESIS AND CHARACTERIZATION OF  
MgO AND MgO/ZnO MULTILAYER THIN FILMS  
FOR HEAT SPREADING APPLICATION IN  
LIGHT EMITTING DIODE PACKAGING**

**IDRIS MUHAMMAD SANI**

**UNIVERSITI SAINS MALAYSIA**

**2021**

**SYNTHESIS AND CHARACTERIZATION OF  
MgO AND MgO/ZnO MULTILAYER THIN FILMS  
FOR HEAT SPREADING APPLICATION IN  
LIGHT EMITTING DIODE PACKAGING**

by

**IDRIS MUHAMMAD SANI**

**Thesis submitted in fulfilment of the requirements  
for the degree of  
Doctor of Philosophy**

**February 2021**

## ACKNOWLEDGEMENT

Alhamdulillah, firstly, I express my utmost gratitude to Allah for the blessing and grace that He has given to me throughout the years of my postgraduate research. Whom provide me with the good health, strength, knowledge, and guidance to complete this thesis. I want to express my sincere gratitude and deep appreciation to my main supervisor, Dr Shanmugan Subramani for his valuable guidance, suggestion, and idea, as well as patience in supporting and motivating me throughout the entire research period. I also give my sincere thanks and appreciation to my co-supervisor's Dr Wan Maryam Wan Ahmad Kamil and Dr Mohd. Zamir Pakhurddin for their guidance and valuable inputs in this research project. I give my special thanks to all lab technicians and staff from the Thermal Management Research lab (TMRL) and Nano Optoelectronics Research Laboratory (NOR) for the endless technical support on the associated research equipment. I would also like to express my profound gratitude to my fellow lab colleagues Anitha, Dheephan, Muna, Jass, Shyma, Nabihah, Hamza El-ladan, Mutawalli, Vishnu, Murali, Vignesh and Puurnaraj. They have been helpful for me during tough times and sharing ideas and experience throughout the research journey. I am incredibly grateful to my friends Abba Aminu Bako, Sirajo Alhassan, Sanusi Dangiwa, Sadik Umar and Aminu Safana for their friendship and hospitality.

Finally, my special thanks and appreciation goes to my loving parents and siblings for their love, patient, prayers, encouragement during my research journey. My extremely gratitude goes to my wife and daughters, Hajia Binta Bashir Yakasai, Fatima Sani Idris and Maimuna Sani Idris for their support, patience, endurance and prayers through the peak and valleys of my postgraduate life.

Thank you.

Idris Muhammad Sani

## TABLE OF CONTENTS

<b>ACKNOWLEDGEMENT</b> .....	<b>ii</b>
<b>TABLE OF CONTENTS</b> .....	<b>iii</b>
<b>LIST OF TABLES</b> .....	<b>ix</b>
<b>LIST OF FIGURES</b> .....	<b>x</b>
<b>LIST OF SYMBOLS</b> .....	<b>xviii</b>
<b>LIST OF ABBREVIATIONS</b> .....	<b>xx</b>
<b>ABSTRAK</b> .....	<b>xxii</b>
<b>ABSTRACT</b> .....	<b>xxiv</b>
<b>CHAPTER 1 INTRODUCTION</b> .....	<b>1</b>
1.1 Introduction to Thermal Management in Electronics Packaging.....	1
1.2 Thermal Management in LEDs .....	3
1.3 MgO/ZnO Multilayer Ceramic-Ceramic Thin Film .....	5
1.4 Problem Statement .....	7
1.5 Objectives.....	9
1.6 Research Contribution.....	9
1.7 Research Novelty .....	11
1.8 Thesis Outline .....	11
<b>CHAPTER 2 LITERATURE REVIEW</b> .....	<b>13</b>
2.1 Overview .....	13
2.2 Thermal management of LEDs .....	13
2.3 Significance of thermal management in electronic and optoelectronic devices.....	17
2.4 Heat transfer through thermal interface materials.....	18
2.4.1 Significance of Thin Film Solid Materials as TIM .....	23
2.4.2 Heat Transfer through Solid Thin Film Thermal Interface Materials.....	24

2.5	MgO and ZnO thin film growth techniques.....	30
2.6	Properties of MgO and ZnO.....	33
2.7	MgO and ZnO Multilayer Growth.....	36
2.8	Theoretical background.....	42
2.8.1	Concept of Thin Film Thickness.....	42
2.8.2	Concept of heat transfer and thermal conductivity of materials.....	44
2.8.3	Heat conduction through thermally conductive solid materials.....	46
2.8.4	Junction temperature, thermal resistance, and thermal impedance.....	48
2.8.5	Thermal, optical, and infrared relation in thermal transient measurements.....	52
<b>CHAPTER 3      METHODOLOGY .....</b>		<b>54</b>
3.1	Overview.....	54
3.2	Preparation of Al (5052 grade) and Cu substrates.....	55
3.3	Preparation of MgO and MgO/ZnO Thin Films.....	56
3.3.1	Synthesis of MgO Sol-Gel Solution.....	56
3.3.2	Spin Coating Process.....	57
3.3.3	Deposition of MgO films, evaporation, and annealing process.....	57
3.4	Preparation of MgO/ZnO Multilayer Thin Films.....	59
3.4.1	Synthesis of MgO/ZnO Sol-Gel Solution.....	59
3.4.2	Deposition of MgO/ZnO Multilayer films, evaporation, and annealing process.....	59
3.5	MgO and MgO/ZnO thin films characterization.....	61
3.5.1	Thin Film Structural Analysis - X-Ray Diffraction.....	62
3.5.2	Surface Morphology - Field Emission Scanning Electron Microscopy (FESEM).....	64
3.5.3	Surface Topography – Atomic Force Microscope (AFM).....	64

3.6	Thermal conductivity and thermal transient analysis.....	66
3.6.1	Thermal conductivity measurement.....	66
3.6.2	Thermal transient measurement of LEDs package .....	69
3.7	Optical Performance and Thermal IR characterization.....	75
3.7.1	Optical performance analysis.....	75
3.7.2	Thermal Infrared Imaging analysis .....	76
<b>CHAPTER 4</b>	<b>RESULTS AND DISCUSSION</b>	
	<b>SYTHESIS OF MgO FILMS ON Al (5052)</b>	
	<b>SUBSTRATES USING SOL-GEL SPIN COATING</b>	
	<b>TECHNIQUE .....</b>	<b>77</b>
4.1	Introduction .....	77
4.2	Growth and analysis of MgO thin film coated Al substrates at different coating cycles .....	77
4.2.1	Structural Analysis .....	78
4.2.1(a)	Film Thickness Measurement.....	81
4.2.1(b)	Surface Morphology Analysis.....	82
4.2.1(c)	Surface Roughness Analysis .....	84
4.2.2	Thermal Transport properties Measurements .....	86
4.2.3	Thermal Transient Characterization of MgO Thin Film as TIM cum Heat Spreader for LEDs Packaging .....	87
4.2.3(a)	Total Thermal resistance for MgO thin film prepared using different coating cycles.....	88
4.2.3(b)	Rise in junction temperature for MgO thin film prepared using different coating cycles.....	90
4.2.3(c)	Thermal Impedance for MgO thin film prepared using different coating cycles.....	91
4.3	Growth and Analysis of MgO Thin Films Coated Al Substrate at Different Coated Films Preheating Time .....	93
4.3.1	Film Thickness Measurement .....	93
4.3.2	Structural Analysis .....	94
4.3.3	Surface Morphology Analysis.....	96

4.3.4	Surface Roughness Analysis .....	98
4.3.5	Thermal Conductivity Measurement.....	100
4.3.6	Thermal Transient Characterization of MgO Thin Film as TIM cum Heat Spreader for LEDs Packaging .....	101
4.3.6(a)	Total Thermal Resistance for LEDs interfaced with MgO Thin Film Preheated for 5, 10, and 20 minutes.....	101
4.3.6(b)	Rise in junction temperature for LEDs mounted on MgO thin film coated Al substrates and preheated at 5, 10, and 20 minutes.....	103
4.3.6(c)	Thermal Impedance for LEDs Mounted on MgO Thin Film Coated Al Substrates and Preheated at 5, 10, and 20 minutes.....	104
4.4	Analysis of MgO Thin Films Coated Al Substrate at Different Annealing Time.....	106
4.4.1	Structural Analysis .....	106
4.4.2	Surface Morphology and Topology of MgO Thin Films at different annealing time .....	109
4.4.2(a)	MgO Film Thickness .....	109
4.4.2(b)	Surface Morphology Analysis.....	110
4.4.2(c)	Surface Roughness Analysis .....	112
4.4.3	Thermal Conductivity Measurement.....	113
4.4.4	Thermal Transient Characterization of MgO Thin Films as TIM cum Heat Spreader in LEDs Packaging.....	114
4.4.4(a)	Total Thermal Resistance for MgO Thin Films Annealed at Different Duration of Time .....	114
4.4.4(b)	Rise in Junction Temperature for MgO Thin Films Annealed at Different Duration of Time .....	116
4.4.4(c)	Thermal Impedance for MgO Thin Films Annealed at Different Duration of Time .....	117
4.5	Growth and Analysis of MgO Thin Films Coated Al Substrate at Different Solution Concentration.....	119
4.5.1	Structural Analysis .....	120

4.5.2	Surface Morphology and Topology of MgO Thin Films at a different solution concentration .....	123
4.5.2(a)	Surface Morphology and Compositional Analysis.....	123
4.5.2(b)	Surface Roughness Analysis .....	125
4.5.3	Thermal Conductivity Measurement.....	127
4.5.4	Thermal Transient Characterization of MgO Thin Films prepared from different molar concentration .....	128
4.5.4(a)	Total Thermal Resistance and a heat spreader to ambient thermal resistance .....	128
4.5.4(b)	Rise in Junction Temperature for LEDs fixed on MgO Thin Films at Different concentration.....	131
4.5.4(c)	Thermal Impedance analysis .....	133
4.6	Summary .....	135
<b>CHAPTER 5</b>	<b>RESULTS AND DISCUSSION</b>	
	<b>SYNTHESIS AND ANALYSIS OF MgO/ZnO</b>	
	<b>MULTILAYER FILMS ON ALUMINUM (Al 5052)</b>	
	<b>AND COPPER (Cu) SUBSTRATES BY SOL-GEL</b>	
	<b>SPIN COATING TECHNIQUE.....</b>	<b>136</b>
5.1	Introduction.....	136
5.2	Comparative study on the structural, surface, and thermal transport properties of MgO and MgO/ZnO multilayer films on Al and Cu substrates.....	137
5.2.1	Structural Analysis.....	138
5.2.2	Surface Morphology and Topology of MgO and MgO/ZnO multilayer Thin Films.....	143
5.2.2(a)	Surface Morphology Analysis.....	143
5.2.2(b)	Surface Roughness Analysis .....	149
5.2.2(c)	Thermal Transport Properties Analysis.....	156
5.3	Comparative study on thermal transient, optical and thermal imaging analysis for LEDs mounted on bare Al, Cu, MgO, and MgO/ZnO multilayer films coated Al and Cu substrates .....	159
5.3.1	Thermal transient analysis.....	160
5.3.1(a)	Total thermal resistance of LEDs on bare and coated substrates .....	160

5.3.1(b)	Rise in junction temperature for LEDs on bare and coated substrates .....	165
5.3.1(c)	Thermal impedance for LEDs on bare and coated substrates .....	169
5.3.2	LEDs Optical Performance Analysis .....	173
5.3.3	LED's Package Infrared Thermal Imaging Analysis .....	177
5.4	Summary .....	180
<b>CHAPTER 6</b>	<b>CONCLUSION .....</b>	<b>181</b>
6.1	Conclusion of the Study .....	181
6.2	Recommendations for Future Work.....	182
	<b>REFERENCES.....</b>	<b>183</b>
	<b>LIST OF PUBLICATIONS</b>	

## LIST OF TABLES

		<b>Page</b>
Table 2.1	Thermal resistance and rise in junction temperature of bare and Al <sub>2</sub> O <sub>3</sub> coated Cu and Al substrates respectively (67,71).....	26
Table 2.2	Thermal performance of solid thin film TIMs prepared using different coating technique.....	27
Table 2.3	Properties of MgO .....	34
Table 2.4	Properties of zinc oxide .....	36
Table 3.1	Monolithic MgO and stacked configuration of MgO and ZnO thin films on Al and Cu substrates .....	61
Table 3.2	<i>k</i> -factor for CREE 9.0 W LED.....	74
Table 4.1	Variations in FWHM and crystallite size with number of coating cycles.....	81
Table 4.2	Thermal transport properties for MgO thin films coated using different coating cycles .....	87
Table 4.3	Thermal transport properties for MgO thin films preheated for 5, 10, and minutes .....	100
Table 4.4	Structural parameter for MgO films at various annealing time .....	108
Table 4.5	Thermal transport properties for MgO thin films annealed for 1, 2, 6, and 10 hour.....	114
Table 4.6	Variation in structural parameters with different solution concentration.....	122
Table 4.7	Thermal transport parameters of bare Al substrate and MgO thin films prepared using different molar concentration .....	128
Table 5.1	Film thickness and structural parameters of MgO and MgO/ZnO multilayer films coated Al substrate .....	141
Table 5.2	Film thickness and structural parameters of MgO and MgO/ZnO multilayer films coated Cu substrate .....	141
Table 5.3	Thermal transport properties for bare, MgO, and MgO/ZnO multilayer thin films coated Al substrates. ....	157
Table 5.4	Thermal transport properties for bare, MgO, and MgO/ZnO multilayer thin films coated Cu substrates.....	157

## LIST OF FIGURES

		<b>Page</b>
Figure 1.1	Showing observation for computing density per unit area continues to increase at a rate of $k^3$ . While the dynamic power density is projected to accelerate anew (from $k^{0.7}$ to $k^{1.9}$ ) [5] .....	2
Figure 1.2	Illustrating (a) irregular surface filled with air and (b) irregular surface filled with thermally conductive thermal interface material [12].....	4
Figure 1.3	Illustration of LED mounted on TIM and showing heat dissipation via (a) the TIM only, (b) the TIM and through the in-plane direction (coated and exposed area to the ambient), (c) top view of Fig. 1.3 (b) .....	10
Figure 2.1	Heat transfer via conduction, convection, and radiation from the LED to the environment [38] .....	15
Figure 2.2	Schematic diagram of heat transfer mechanism from LED package to the ambient [41].....	16
Figure 2.3	Schematic illustration of TIM filling in the air gap between LED package and heat sink .....	18
Figure 2.4	Model diagram for contact thermal resistance for LED, TIM and heat-sink set up .....	20
Figure 2.5	Basic phases to spin coating process .....	31
Figure 2.6	Schematic illustration of phases involved in thin film synthesis using spin coating technique .....	32
Figure 2.7	Schematic illustration of MgO cubic structure .....	33
Figure 2.8	Schematic illustration of ZnO crystal structures [196].....	35
Figure 2.9	Schematic illustration of spinning disk used by Emslie model, the rotational plane is horizontal.....	43
Figure 2.10	One- dimensional heat flow by conduction .....	46
Figure 2.11	Schematic illustration of two bodies in contact and heat flow across the interface, (a) with air or thermal paste and (b) with metal (Al or Cu) coated with thermally conductive material and sandwiched between the contacting surfaces.....	48
Figure 2.12	Models of (a) thermal resistor of an LED fixed on a heat sink [38] and (b) Foster-Cauer thermal network. ....	49

Figure 2.13	Typical illustration of cumulative structure function extracted from thermal transient analysis and its equivalent Foster-Cauer RC thermal network [138].	50
Figure 3.1	Comprehensive flow chart of the research methodology	55
Figure 3.2	Flow chart illustration of sol-gel solution preparation and MgO thin films deposition process	58
Figure 3.3	Flow chart diagram for MgO and ZnO sol-gel preparation and MgO/ZnO multilayer thin films deposition process	60
Figure 3.4	Illustrating the stacking sequence of MgO/ZnO multilayer	61
Figure 3.5	Thermal conductivity measurement set-up (a) sensor and other apparatus, (b) Kapton placed between two identical coated Al substrates, (c) complete schematic TPS Hot Disc thermal analyzer set up	68
Figure 3.6	T3Ster setup for thermal measurement	69
Figure 3.7	Illustration of thermal transient modeling (a) LED set-up (b) transient cooling curve and (c) equivalent Foster-Cauer RC thermal network	70
Figure 3.8	Thermal transient measurement setup (a) the Booster and thermostat, (b) DUT placed inside thermostat, (c) and stages illustration on how LED is fixed to different boundary conditions	72
Figure 3.9	Graph of voltage drop against ambient temperature (( $k$ -factor) of tested LED)	74
Figure 3.10	Handheld spectrometer placed on still air box while the LED is switched on inside the box	75
Figure 3.11	IR thermal image experimental setup	76
Figure 4.1	XRD pattern of MgO thin film on Al substrate at different number of coating cycles	79
Figure 4.2	Enlarge XRD pattern of MgO thin film on Al substrate at different number of coating cycles	80
Figure 4.3	Cross-sectional FESEM images of MgO films	82
Figure 4.4	FESEM surface morphology of MgO thin films at different number of coating cycles	83
Figure 4.5	Graph of average grain size of MgO thin films at different coating cycles	84

Figure 4.6	3D AFM images of MgO thin film deposited using different coating cycles.....	85
Figure 4.7	Surface roughness for MgO thin films coated using different coating cycles.....	86
Figure 4.8	Cumulative structure-function for LEDs attached to different layers MgO thin film coated Al substrates .....	89
Figure 4.9	Total thermal resistance of LEDs attached to different layers MgO thin film .....	89
Figure 4.10	Smooth response for LEDs attached to MgO thin film coated Al substrate using 5, 10, 15, and 20 coating cycles .....	90
Figure 4.11	Rise in junction temperature for LEDs fixed to MgO thin films deposited using different coating cycles.....	91
Figure 4.12	Structure function (thermal impedance) of LED fixed to MgO thin film prepared using different coating cycles.....	92
Figure 4.13	Thermal impedance for LEDs fixed on MgO thin films deposited using different coating cycles.....	92
Figure 4.14	Cross-sectional image of MgO film grown at different preheating time .....	94
Figure 4.15	XRD pattern of MgO thin film on Al substrate at different film preheating time.....	95
Figure 4.16	FESEM surface morphology of MgO thin films deposited at different preheating time.....	97
Figure 4.17	Relationship between grain size of MgO thin films and film preheating time .....	97
Figure 4.18	3D AFM images of MgO thin film deposited using different film preheating time.....	99
Figure 4.19	Surface roughness for MgO films coated Al substrate at different film preheating time.....	99
Figure 4.20	Cumulative structure-function for LEDs mounted on MgO thin film coated Al substrates and preheated at 5, 10, and 20 minutes.....	102
Figure 4.21	Total thermal resistance for LEDs mounted on MgO thin film coated Al substrates and preheated at 5, 10, and 20 minutes.....	102

Figure 4.22	Smooth response for LEDs mounted on MgO thin film coated Al substrates and preheated at 5, 10, and 20 minutes.....	103
Figure 4.23	Rise in junction temperature for LEDs mounted on MgO thin film coated Al substrates and preheated at 5, 10, and 20 minutes.....	104
Figure 4.24	Structure function (thermal impedance) for LEDs mounted on MgO thin film coated Al substrates and preheated at 5, 10, and 20 minutes.....	105
Figure 4.25	Thermal impedance for LEDs mounted on MgO thin film coated Al substrates and preheated at 5, 10, and 20 minutes.....	105
Figure 4.26	XRD pattern of MgO thin film on Al substrate at various annealing time.....	108
Figure 4.27	FESEM cross-sectional images of MgO film grown at different annealing time.....	109
Figure 4.28	FESEM surface morphology of MgO thin films annealed at different duration.....	111
Figure 4.29	Relationship between annealing period and MgO thin films grains size.....	111
Figure 4.30	3D AFM images of MgO thin film synthesized and annealed at different duration.....	112
Figure 4.31	Variation in surface roughness for MgO films annealed at different duration.....	113
Figure 4.32	Cumulative structure-function for LEDs attached to MgO thin film coated Al substrate and annealed at 600 °C at 1, 2, 6 and 10 hour.....	115
Figure 4.33	Total thermal resistance of MgO thin film annealed at different duration of time.....	116
Figure 4.34	Smooth response for LEDs attached to MgO thin film coated Al substrate and annealed at 600 °C at 1, 2, 6 and 10 hour.....	117
Figure 4.35	Rise in junction temperature for LEDs fixed to MgO thin films annealed at different duration.....	117
Figure 4.36	Structure function (thermal impedance) for LEDs mounted on MgO thin film annealed for 1, 2, 6, and 10 hour.....	118

Figure 4.37	Thermal impedance for LEDs mounted on MgO thin film annealed for 1, 2, 6, and 10 hour .....	119
Figure 4.38	XRD pattern of MgO thin film on Al substrate at different solution concentration.....	121
Figure 4.39	Enlarge XRD pattern of MgO thin film on Al substrate at different solution concentration.....	122
Figure 4.40	Cross-sectional image of MgO thin films prepared using different concentration.....	124
Figure 4.41	FESEM surface morphology of MgO thin films deposited using different concentration .....	124
Figure 4.42	Average grain size of MgO films at different precursor concentration.....	125
Figure 4.43	3D AFM images of MgO thin films at different concentration.....	126
Figure 4.44	Surface roughness values for MgO thin films at different solution concentration.....	126
Figure 4.45	Cumulative structure-function for LEDs attached to MgO thin film prepared from different molar concentration (0.2, 0.4, 0.6, 0.8 and 1.0 M).....	129
Figure 4.46	Total thermal resistance for LEDs fixed on MgO thin film deposited at different concentration.....	130
Figure 4.47	Thermal resistance for proposed MgO thin film heat spreader.....	130
Figure 4.48	Smooth response for LEDs attached to MgO thin film prepared from different molar concentration (0.2, 0.4, 0.6, 0.8 and 1.0 M).....	132
Figure 4.49	Rise in junction temperature for LEDs fixed on bare, commercial thermal pad and MgO thin films at different concentrations .....	132
Figure 4.50	Structure function (thermal impedance) extracted from transient cooling curve of LED fixed to MgO thin film prepared from different molar concentration (0.2, 0.4, 0.6, 0.8 and 1.0 M).....	134
Figure 4.51	Thermal impedance for LEDs fixed on bare Al, commercial thermal pad, and MgO thin films at different solution concentration.....	134

Figure 5.1	XRD pattern of MgO and MgO/ZnO thin films coated Al substrate .....	139
Figure 5.2	XRD pattern of MgO and MgO/ZnO thin films coated Cu substrate .....	140
Figure 5.3	FESEM surface morphology of MgO and MgO/ZnO thin films deposited on Al substrates .....	145
Figure 5.4	FESEM surface morphology of MgO and MgO/ZnO thin films deposited on Cu substrates .....	146
Figure 5.5	Cross-sectional images of MgO and MgO/ZnO multilayer thin films from FESEM images analysis .....	146
Figure 5.6	Average grain size for MgO and MgO/ZnO coated Al and Cu substrates .....	147
Figure 5.7	EDX of MgO and MgO/ZnO multilayer thin films on Al substrates.....	148
Figure 5.8	EDX of MgO and MgO/ZnO multilayer thin films on Cu substrates.....	148
Figure 5.9	3D AFM images of MgO and MgO/ZnO multilayer thin films coated Al substrates .....	150
Figure 5.10	3D AFM images of MgO and MgO/ZnO multilayer thin films coated Cu substrates .....	151
Figure 5.11	Surface roughness and peak-valley profile of bare Al, MgO and MgO/ZnO thin films coated Al substrates .....	153
Figure 5.12	Surface roughness and peak-valley profile of bare Cu, MgO, and MgO/ZnO thin films coated Cu substrates.....	153
Figure 5.13	Peak-valley distance for MgO and MgO/ZnO multilayer thin films coated Al substrate .....	155
Figure 5.14	Peak-valley distance for MgO and MgO/ZnO multilayer thin films coated Cu substrates .....	156
Figure 5.15	Cumulative structure function for LED mounted on the bare, commercial pad and Al coated substrates.....	160
Figure 5.16	Total thermal resistance for high-power LED mounted on bare Al, commercial pad and MgO and MgO/ZnO thin film coated Al substrates .....	161
Figure 5.17	Heat spreader thermal resistance for high-power LED mounted on bare Al, commercial pad and MgO and MgO/ZnO thin film coated Al substrates .....	161

Figure 5.18	Cumulative structure function for LED mounted on the bare, commercial pad and Cu coated substrates .....	164
Figure 5.19	Total thermal resistance for high-power LED mounted on bare Cu, commercial pad and MgO and MgO/ZnO thin film coated Cu substrates .....	164
Figure 5.20	Heat spreader thermal resistance for high-power LED mounted on bare Cu, commercial pad and MgO and MgO/ZnO thin film coated Cu substrates.....	165
Figure 5.21	Smooth response for LEDs attached to bare, commercial thermal pad, monolithic MgO and MgO/ZnO multilayer thin film coated Al substrates .....	166
Figure 5.22	Smooth response for LEDs attached to bare, commercial thermal pad, monolithic MgO and MgO/ZnO multilayer thin film coated Cu substrates.....	166
Figure 5.23	Rise in junction temperature, $T_J$ ( $^{\circ}\text{C}$ ) for high-power LED mounted on bare Al, commercial pad, MgO and MgO/ZnO thin film coated Al substrates .....	167
Figure 5.24	Rise in junction temperature, $T_J$ ( $^{\circ}\text{C}$ ) for high-power LED mounted on bare Cu, commercial pad, MgO and MgO/ZnO thin film coated Cu substrates.....	167
Figure 5.25	Structure function for LEDs attached to bare, commercial thermal pad, monolithic MgO and MgO/ZnO multilayer thin film coated Al substrates .....	170
Figure 5.26	Structure function for LEDs attached to bare, commercial thermal pad, monolithic MgO and MgO/ZnO multilayer thin film coated Cu substrates.....	170
Figure 5.27	Thermal impedance $Z_{th}$ ( $^{\circ}\text{C}$ ) for high-power LEDs mounted on bare Al, commercial thermal pad, MgO and MgO/ZnO multilayer thin films coated Al substrates .....	171
Figure 5.28	Thermal impedance $Z_{th}$ ( $^{\circ}\text{C}$ ) for high-power LEDs mounted on bare Cu, commercial thermal pad, MgO and MgO/ZnO multilayer thin films coated Cu substrates.....	172
Figure 5.29	CCT behaviour for LEDs mounted on bare Al, commercial pad, MgO and MgO/ZnO thin film coated Al substrates .....	174
Figure 5.30	CCT behaviour for LEDs mounted on bare Cu, commercial pad, MgO and MgO/ZnO thin film coated Cu substrates.....	175
Figure 5.31	LUX behaviour for LEDs mounted on bare Al substrate, commercial pad, MgO and MgO/ZnO thin film coated Al substrates.....	176

Figure 5.32	LUX behaviour for LEDs mounted on bare Cu substrate, commercial pad, MgO and MgO/ZnO thin film coated Cu substrates.....	176
Figure 5.33	IR images for surface temperature ( $T_s$ ) for LEDs mounted on bare Al, commercial thermal pad, MgO and MgO/ZnO multilayer thin film coated Al substrates.....	177
Figure 5.34	Showing IR surface temperature ( $T_s$ ) profile from the top view of LEDs mounted on different boundary conditions and run for 0, 10, 20 and 30 minutes .....	178
Figure 5.35	IR images for surface temperature ( $T_s$ ) for LEDs mounted on bare Cu, commercial thermal pad, MgO and MgO/ZnO multilayer thin film coated Cu substrates .....	179
Figure 5.36	Showing IR surface temperature ( $T_s$ ) profile from the top view of LEDs mounted on different boundary conditions and run for 0, 10, 20 and 30 minutes .....	180

## LIST OF SYMBOLS

$A$	Cross-sectional area
$a, c$	Lattice constant
$C_p$	Specific heat capacity
$D$	Crystallite size
$K$	Thermal conductivity
$K_{TIM}$	Thermal Conductivity of Thermal Interface Material
$L$	Length
$P_H$	Heat dissipation
$Q$	Heat flow
$q$	Heat transfer rate
$R_{bulk}$	Thermal resistance of TIM because of BLT, $K$ and $R_c$
$R_c$	Contact resistance
$R_{effective}$	Effective thermal resistance at the interface
$R_{th}$	Thermal Resistance
$R_{th-Ambient}$	Al/Cu substrate to ambient thermal resistance
$R_{th-TIM}$	TIM thermal resistance
$R_{th-tot}$	Total thermal resistance
$T$	Temperature
$T_J$	Junction Temperature
$T_{j0}$	Initial junction temperature
$T_S$	Surface temperature
$\Delta R_{th}$	Difference in thermal resistance
$\Delta T_J$	Difference in rise in junction temperature
wt %	Weight percentage
vol%	Volume percentage

$\%$	Percentage
$Z_{th}$	Thermal impedance
$\beta$	Full width at half maximum (FWHM)
$\Delta$	Difference
$\delta$	Dislocation density
$\Delta R_{th}$	Difference in thermal resistance
$\Delta T_j$	Difference in rise in junction temperature
$\varepsilon$	Strain
$\theta$	Bragg diffraction angle
$\lambda$	Wavelength

## LIST OF ABBREVIATIONS

AFM	Atomic force microscopy
Ag	Silver
Al	Aluminum
ASTM	American Society for Testing and Materials
<i>BLT</i>	Bond Line Thickness
BN	Boron Nitride
CCT	Correlated colour temperature
CNT	Carbon Nanotubes
CRI	Colour rendering index
CSF	Cumulative Structure function
Cu	Copper
CVD	Chemical Vapor Deposition
DUT	Device under test
EDX	Energy Dispersive X-Ray Analysis
FESEM	Field emission scanning electron microscopy
FWHM	Full width half maximum
IR	Infrared
JEDEC	Joint electron device engineering council
LED	Light Emitting Diode
LUX	Illuminance
MCPCB	Metal core printed circuit board
MgO	Magnesium oxide
MOCVD	Metal organic chemical vapor deposition
O/O <sub>2</sub>	Oxygen
PCB	Printed circuit board

PCM	Phase change materials
RMS	Root mean square
RPM	Revolutions per minute
SiC	Silicon carbide
SiO <sub>2</sub>	Silicon dioxide
T3ster	Thermal transient tester
TIMs	Thermal interface materials
UV	Ultraviolet
XRD	X-ray diffraction
ZAD	Zinc acetate dihydrate
Zn	Zinc
ZnO	Zinc Oxide
3D	Three dimensional

**SINTESIS DAN PENCIRIAN FILEM NIPIS MgO DAN MgO/ZnO  
PELBAGAI LAPIS UNTUK APLIKASI PENYEBARAN HABA DALAM  
PEMBUNGKUSAN DIOD PEMANCAR CAHAYA**

**ABSTRAK**

Penyelidikan ini dijalankan untuk mensintesis filem nipis pelbagai lapisan magnesium oksida (MgO) dan magnesium oksida - zink oksida (MgO/ZnO) sebagai pelepasan haba atau TIM untuk pengurusan haba yang cekap dalam sistem pembungkusan LED. Filem nipis MgO (10 lapisan) dan MgO/ZnO pelbagai lapisan (disusun secara berasingan dalam konfigurasi lapisan 9:1, 8:2, 7:3, 6:4 dan 5:5) disaluti atas substrat aluminium (gred Al 5052) dan kuprum (Cu) dengan menggunakan teknik pelapisan putaran. Pada bahagian pertama, filem nipis MgO adalah disintesis dengan menggunakan 0.6 M, 10 kitaran salutan, dipanaskan pada suhu 200 °C selama 20 minit, dan akhirnya dipanaskan pada 600 °C selama 1 jam. Pencirian struktur oleh XRD menunjukkan kehadiran fasa (200), (220), dan (222) MgO dengan ukuran saiz kristal (37.47 nm), pengurangan mikrostrain ( $2.5 \times 10^{-3}$ ) dan ketumpatan dislokasi ( $7.0 \times 10^{-4}$  baris/m<sup>2</sup>) untuk 0.6 M MgO bersalut Al. Saiz butiran pengedaran seragam adalah 74 nm dan kekasaran permukaan 19.11 nm disahkan oleh analisis FESEM dan AFM. Perbezaan yang signifikan dalam suhu persimpangan ( $\Delta T_J = 24.7\%$ ) dan rintangan haba total ( $\Delta R_{th-tot} = 3.86$  K/W) dicatatkan untuk LED yang dipasang pada filem 0.6 M MgO bersalut Al berbanding dengan Al sahaja. Pada bahagian kedua, ZnO ditambahkan ke MgO monolitik untuk memperbaiki sifat pengangkutan struktur, permukaan, dan termal filem MgO. Antara pelbagai lapisan MgO/ZnO yang dikaji, MgO/ZnO 6:4 L memaparkan saiz kristal yang lebih besar iaitu 52 nm (Al) dan 35 nm

(Cu) dengan keberkonduktan haba 24.31 W/mK (Al), dan 15.13 W/mK (Cu)) masing-masing. Filem pelbagai lapisan 6:4 L MgO/ZnO menunjukkan kekasaran permukaan yang lebih rendah (9.6 nm (Al) dan 2.6 nm (Cu)) dengan butiran yang diedarkan secara seragam dan kehadiran sebilangan besar titik sentuhan kepada pakej LED. Difusiviti terma tertinggi 0.4796 mm<sup>2</sup>/s (Al) dan 0.4466 mm<sup>2</sup>/s (Cu) dan nilai terendah bagi muatan haba tentu 51.79 Jmol<sup>-1</sup>K<sup>-1</sup> (Al) dan 33.87 Jmol<sup>-1</sup>K<sup>-1</sup> (Cu) dicatatkan untuk 6:4 L MgO/ZnO pelbagai lapisan. Perbezaan yang lebih ketara dalam R<sub>th-tot</sub> (5.31 K/W untuk Al dan 3.18 K/W untuk Cu) dan penurunan pengurangan T<sub>J</sub> yang ketara (27% dari Al dan 25% dari sampel Cu), peningkatan 12% dan 10.7% dari terma impedans untuk lapisan 6:4 L (MgO:ZnO) yang disalut atas substrat Al dan Cu. Output optik LED yang lebih baik dan penlesapan haba yang cekap (analisis pencitraan IR) direkodkan untuk pelbagai lapisan 6:4 L. Secara keseluruhannya, substrat Al bersalut lapisan pelbagai MgO/ZnO (6:4 L) menunjukkan prestasi yang baik dalam meningkatkan prestasi terma dan output optik LED.

**SYNTHESIS AND CHARACTERIZATION OF MgO AND MgO/ZnO  
MULTILAYER THIN FILMS FOR HEAT SPREADING APPLICATION IN  
LIGHT EMITTING DIODE PACKAGING**

**ABSTRACT**

This research was carried out to synthesize magnesium oxide (MgO) and magnesium oxide - zinc oxide (MgO/ZnO) multilayer thin film as a TIM cum heat spreader for efficient thermal management in LEDs packaging system. MgO (10 layers) and MgO/ZnO multilayer (stacked separately in a configuration of 9:1, 8:2, 7:3, 6:4 and 5:5 layers) thin films are coated over aluminum (Al 5052 grade) and copper (Cu) substrates using spin coating technique. In the first part, MgO thin film was synthesis using 0.6 M, 10 coating cycles, preheated at 200 °C for 20 minutes, and finally annealed at 600 °C for 1 hour. Structural characterization by XRD shows the presence of (200), (220), and (222) MgO phases with crystalline size (37.47 nm), reduced microstrain ( $2.5 \times 10^{-3}$ ) and dislocation density ( $7.0 \times 10^{-4}$  lines/m<sup>2</sup>) for 0.6 M MgO coated Al. Uniform distribution of 74 nm size grains and surface roughness of 19.11 nm were confirmed by FESEM and AFM analysis. A significant difference in junction temperature ( $\Delta T_J = 24.7\%$ ) and total thermal resistance ( $\Delta R_{th-tot} = 3.86$  K/W) were recorded for LED fixed on 0.6 M MgO coated Al compared to that of bare Al. In the second part, ZnO was added to the monolithic MgO to improve the structural, surface, and thermal transport properties of MgO. Among the studied MgO/ZnO multilayers, 6:4 L MgO/ZnO displayed larger crystalline sizes of 52 nm (Al) and 35 nm (Cu) with thermal conductivity of 24.31 W/mK (Al), and 15.13 W/mK (Cu) respectively. 6:4 L MgO/ZnO multilayer films showed lower surface roughness (9.6

nm (Al) and 2.6 nm (Cu)) with uniformly distributed grains and presence of large numbers of contact points to the LEDs package. The highest thermal diffusivity 0.4796 mm<sup>2</sup>/s (Al) & 0.4466 mm<sup>2</sup>/s (Cu) and the lowest value of specific heat capacity 51.79 Jmol<sup>-1</sup>K<sup>-1</sup>(Al) and 33.87 Jmol<sup>-1</sup>K<sup>-1</sup> (Cu) were recorded for 6:4 L MgO/ZnO multilayers. A more significant difference in  $R_{th-tot}$  (5.31 K/W for Al and 3.18 K/W for Cu) and considerable reduction in  $T_J$  reduction (27% from Al and 25% from Cu samples), 12% and 10.7% improvement from thermal impedance for 6:4 L (MgO:ZnO) layers deposited Al and Cu substrates. An improved optical output of LED and efficient heat distribution (IR imaging analysis) was recorded for 6:4 L multilayers. Overall, MgO/ZnO (6:4 L) multilayer coated Al substrate performed well in improving the thermal performance and optical output of the LED.

# CHAPTER 1

## INTRODUCTION

### 1.1 Introduction to Thermal Management in Electronics Packaging

Continuous miniaturization of electronic chips over the years has made the technology to record advancement in reducing the size of electronic systems. The advance technology reduces the sizes of aerospace technology, lighting systems, microelectronics technology and hybrid data centers to more portable and friendly. Miniaturization of the modern devices has made them more compact, consequently, the number of power-delivery components and their power density to be increasing per square inch on printed circuit board (PCB), thereby twofold the data density within the devices [1, 2]. Similarly, continuous miniaturization of electronics and lighting devices advances the density of the power-delivery components to cover 45-50% of the PCB. The increased power-delivery components create high heat flux which in returns slow down the speed of the devices, deterioration of the device components and overall failure of the parent device [2, 3]. In years to come, it has predicted that power-delivery components density will rise exponentially by 15%, resulting to intensive increase in heat flux [4, 5], which necessitate the thermal management of electronics and lighting devices to be addressed, to avoid escalation of the device. Figure 1.1 illustrates future projection in power density [5]. As such, electronics and lighting industries focused on addressing thermal management challenges to develop sustainable devices that have a long lifespan, reliability as well as steady performance.

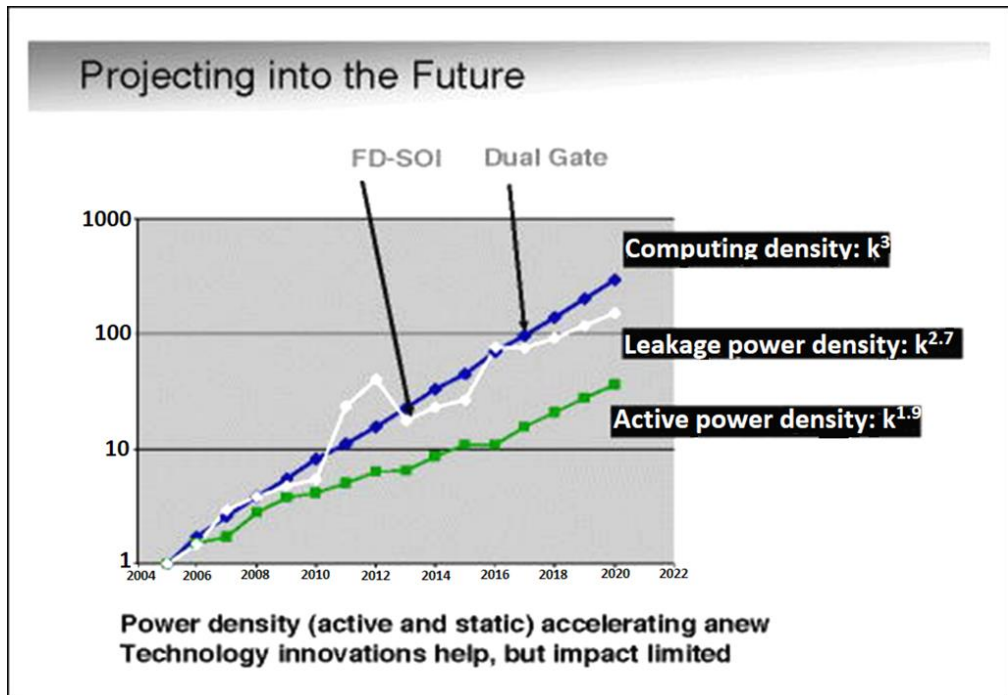


Figure 1.1 Showing observation for computing density per unit area continues to increase at a rate of  $k^3$ . While the dynamic power density is projected to accelerate anew (from  $k^{0.7}$  to  $k^{1.9}$ ) [5]

Nowadays, researches are going on how to come up with a reliable thermal path for electronic devices and address their fatal failure due to thermal runaway. Designing new lighting and electronics thermal path components and improving the existing ones is expected to enhance the rate of heat flux dissipation from the light and electronic devices to ambient efficiently. Therefore, thermal path innovation from highly thermally conductive materials with minimal cost and less complications during application is demanded in electronic device packaging. The thermal path innovation is demanded by manufacturing industries for the present and future miniaturization advancements of optoelectronics devices.

## 1.2 Thermal Management in LEDs

Demands for friendly lighting in different locations such as illuminating foods, streets, automobile, road symbols, architectural, fabrics display stores, airplanes, interior decorations, interior, and exterior lighting have rapidly been increasing for the past two decades. Meanwhile, the usage of conventional sources of light in such locations is causing a lot of damages [6 – 8]. To meet these demands, light emitting diodes (LEDs) from solid-state lighting devices were designed and suggested to be used in these locations because they are cool to the touch and non-generation of infrared (IR) [6]. This makes the lighting industries over the years to develop and design new brands of LEDs to replace the incandescent lamps, compact fluorescent lamps (CFL) and other traditional lighting sources [8 – 11]. LEDs from solid-state lighting technology are designed with some improved features such as more compact, reliability, high luminous flux, excellent color saturation, low input power demand, longer lifespan ( $> 50,000$  hours), eco-friendly and inexpensive. Moreover, LEDs can also have been designed with flexibility, and rugged body that enables their application either in simple or complex locations/parts and they are designed in different shape and sizes, so they are directional to the exact point of the need [8 – 11].

Despite these milestone achievements in power electronics technology, increase from low to high operating power of LEDs leads to increase in heat flux generation thus increasing the phonon dispersing rate and cause a rise in junction temperature ( $T_J$ ) of the LED. The increase in junction temperature will lead to shifts in output wavelength, thermal runaway, failure of the device carrier mobility, shortening of the LED lifetime, decrease in both forward voltage and brightness output as well as rapid deterioration of the LED [8, 9]. Heat flux generated within the LEDs package must be dissipated to the environment effectively to lower  $T_J$  and the keep the

temperature of the device within safe operating limits. Among the parameters that qualify LEDs to be reliable, the  $T_J$  and the total thermal resistance ( $R_{th-tot}$ ) of the package are the key players, and they must be kept at a low level during the operating times [8]. One of the most fundamental challenges in reducing  $T_J$  and  $R_{th}$  is the surface irregularities that exist between the interface of two solid contact surfaces [12]. Figure 1.2 demonstrate the surface irregularities that exist between two solid objects directly in contact and how the irregularities are eliminated by inserting TIM in-between the objects [12]. The irregular surface was filled with air, and the air will restrict the flow of heat and hence poor thermal conduction which causes the rise in  $T_J$  and  $R_{th-tot}$ .

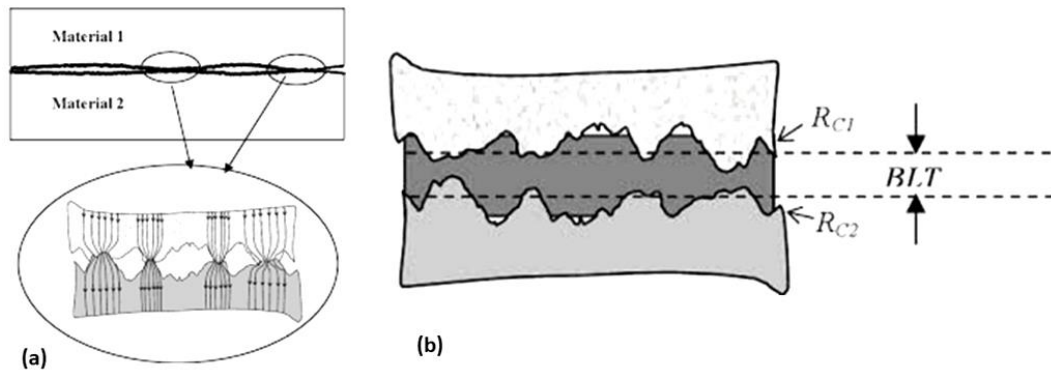


Figure 1.2 Illustrating (a) irregular surface filled with air and (b) irregular surface filled with thermally conductive thermal interface material [12]

To achieve excellent thermal contact conductance and reduction in thermal contact resistance in the solid interface, air gaps generated between two solid contact surfaces must be eliminated and filled with materials such as thermal interface materials (TIMs), heat spreader, die attachments and thermal conductivity grease. Doing so will enhance heat dissipation and lower the  $T_J$  and  $R_{th}$  of the device [12].

Metal oxides and nitrides such as BeO, MgO, Al<sub>2</sub>O<sub>3</sub>, SiO, ZnO, BN and AlN with high thermal conductivity and electrically insulative properties are used in the form of particles as inorganic fillers in epoxy resin or in the form of thin films over

metal substrates as TIM/heat spreader for improving the thermal path between LEDs and heat sink towards convenient removal of high heat flux to the ambient. Those oxides or nitrides are used due to their capability in increasing energy absorption, wide bandgap, insulation properties, excellent thermal and chemical stability, as well as improving both the thermal conductivity of the epoxy resin or that of the metal substrate respectively [1, 13, 14]. However, those ceramic materials are having some drawback associated with them despite their excellent thermal transport properties. For instance, *h*-BN, AlN and BeO have thermal conductivity >200 W/mK; however they have some limitations in their usage as TIM associated to their high cost, high temperature demand during synthesis and health hazard especially with BeO [14]. Al<sub>2</sub>O<sub>3</sub> is an abrasive ceramic material due to its hardness, thereby making it unreliable in the presence of high pressure. Also, Al<sub>2</sub>O<sub>3</sub> is molded under the low shear condition and then possess small filler loading proportion [14]. SiO<sub>2</sub> poses low thermal conductivity (14 W/mK), making it difficult to improve the thermal conductivity of the composite materials significantly, while ZnO is a semiconductor and could be considered as a susceptor [14]. Therefore, the need arises to think of improving the presently used design and providing a suitable alternative proposal.

### **1.3 MgO/ZnO Multilayer Ceramic-Ceramic Thin Film**

Magnesium oxide is a metal oxide that has gained a lot of attention of researchers and industries in recent time because of their attainable properties and potential applications when used as inorganic filler in epoxy resin and employed as TIM or heat spreader in lighting and electronics packaging [13 – 15]. High thermal conductivity (45 W/mK) at room temperature, wide bandgap (7.8 eV), highly insulative, dielectric constant (9.8), nontoxic, excellent chemical properties and

thermally stable up to a temperature level of 371 °C have made MgO a promising candidate for heat dissipation from the LEDs and electronics components [15 – 18]. However, MgO has rarely been utilized as TIM or heat spreader in thermal management of LEDs or electronic components due to its non-favorable mechanical properties and a high coefficient of thermal expansion ( $10 \times 10^{-6} \text{ C}^{-1}$ ) which make MgO have weak thermal shock resistance [19, 20,]. Experiments had proven ceramic-ceramic composites to have exceptional mechanical properties compared to monolithic ceramics, which makes them potential candidates in lighting and electronics packaging and other related high temperature applications [19 – 23]. ZnO is selected in this research to be added to MgO due to their similarity's radii, and the thermodynamic solid solubility of MgO in ZnO is less than 4 mol%. Therefore, the introduction of (ZnO) into MgO will reinforce the mechanical and thermal properties of MgO, improve the structural properties of MgO, surface quality, and develop densification together with hot strength features of the composite MgO/ZnO [23, 24], ZnO has excellent properties, such as low coefficient of thermal expansion ( $4.77 \times 10^{-5} \text{ C}^{-1}$ ), relatively high thermal conductivity (37 W/mK), large exciton binding energy (60 meV), specific heat capacity (40.3 J/mol K) and wide bandgap (3.3 eV) [19, 22, 24].

Similarly, the ZnO is expected to decrease the coefficient of thermal expansion of the composite ceramic, improve the thermal shock resistance, thermal properties as well as strengthen and fracture toughness of the MgO composite. Nowadays, MgO and ZnO multilayer of ceramic-ceramic composite has attracted much attention in restructuring devices features and upgrading their performance [16, 22]. The MgO/ZnO multilayer is designed in the form of thin films which will provide uniform coating, thickness control, and strong adhesion to different types of substrates compared.

Various growth techniques such as electrochemical deposition, RF sputtering, chemical bath, chemical vapor deposition, sol-gel spin coating and spray pyrolysis can be used in depositing MgO/ZnO multilayer thin films on different types of substrates [22]. Efforts are still in progress towards improving the crystalline quality, structural, thermal, and mechanical properties of monolithic MgO and MgO/ZnO multilayer thin films using different deposition techniques.

#### **1.4 Problem Statement**

Continuous reduction of package size in LEDs into a more compactable one, increasing their output power, complete removal of the excessive heat generated within them and keeping the LED's package temperature at an ideal level is demanded by their end-users. These will bring about the compatibility of the modified package and improve the LEDs performance. However, some drawback is being faced by the lighting industries in the sector of thermal management such as: Increase in driving current and miniaturization of LEDs do improve not only their output power but also cause the generation of high heat flux. If this high heat flux not appropriately removed, it would cause a rise in junction temperature ( $T_j$ ), thermal resistance ( $R_{th}$ ) and rapid deterioration of the LEDs [6, 7, 25, 26]. In addition to this, the available commercial TIMs such as thermal paste, thermal pad, thermal adhesive, phase change materials, thermal grease, and solid thin film are associated with some problems of such as low thermal conductivity, high material thickness, pump out for thermal pad, dry out for thermal paste and grease. This make the commercial TIMs be less efficient in improving heat dissipation from the LEDs package, and therefore causes an eventually increase in the junction temperature of the devices when it is operated with Commercial TIMs at higher currents [27, 28]. Therefore, need arises to use a reliable

TIM or heat spreader at the bottom of LEDs to faster transfer of the massive heat flux to the ambient.

One of the major challenges affecting the rate of heat transfer between LED and heat sink is their respective surface irregularities. Air gap is produced due to the surface irregularities at the interface, this causes poor heat dissipation rate by low thermal conductivity of the air molecules. Therefore, need arises to fill the air gap with a thermally conductive solid thin film. This will improve heat dissipation and provide thermal stability within the interface.

Due to the high thermal properties, BN, AlN, SiC, MgO, Al<sub>2</sub>O<sub>3</sub>, SiO<sub>2</sub>, or ZnO were put into use as TIMs, heat spreaders or electronic substrates in LEDs thermal management and electronics packaging for heat dissipation improvement. Despite the excellent performance of BN, AlN, and SiC, their utilization is always discouraging because they are difficult to deposit, high-cost implications and they easily oxides if proper precautions were not taken. While metal oxides based solid thin films have significant advantages such as low cost of production, high quality films, environmentally friendly and simple production process, making them valuable for efficient heat dissipation in LEDs and electronics packages. Among the oxides, MgO and ZnO are selected to overcome health hazard challenges associated with BeO, high temperature demand for synthesizing BN, AlN and SiC, abrasive nature of Al<sub>2</sub>O<sub>3</sub> and low thermal conductivity of Al<sub>2</sub>O<sub>3</sub> and SiO<sub>2</sub>.

MgO and MgO/ZnO solid thin films TIMs cum heat spreader are proposed as an alternative TIMs to overcome present thermal conductivity and poor heat dissipation challenges faced by commercial thermal TIMs and thick films. The aim is to design and synthesize heat spreader materials with an optimum thickness (between 400 - 800 nm) that have a high impact on improving heat dissipation.

## 1.5 Objectives

- i. To synthesize and optimize high-quality MgO and MgO/ZnO multilayer thin films on Al and Cu substrates using a sol-gel spin coating method for achieving higher thermal conductivity and reliable TIM cum heat spreader for effective heat spreading purpose
- ii. To study and optimize the influence of ZnO diffusion into MgO on reshaping the surface of MgO for achieving thin films with low surface roughness. This will improve contact rate between the LED and heat sink and significantly improves heat dissipation.
- iii. To synthesize metal oxide thin film TIM cum heat spreader for cost of production and energy demand reduction. Additionally, to apply and study the optimized multilayer MgO/ZnO composite thin film as TIM cum heat spreader for effective heat dissipation in LEDs and achieving lower device  $T_J$  and  $R_{th-tot}$  values and improving the thermal and optical performance of LEDs.
- iv. To analyze and evaluate the compatibility and performance of the proposed MgO/ZnO composite thin film as solid TIMs cum heat spreader for efficient thermal management in electronic packaging application.

## 1.6 Research Contribution

The contribution of this research is to improve the rate of heat dissipation from the LED's packages to the ambient through a combination of TIM and heat spreading process. Figure 1.3 illustrates the existing heat dissipation process via TIMs medium only and our proposed process which combines two heat transfer media (TIM cum

heat spreader). During any heat transfer through TIM, the change in interface temperature between the LED package and film coated substrates will be minimum (Fig. 1.3 (a)) as it will try to meet the equilibrium state, therefore there is said to be a limited heat transfer rate. If the coating area is extended as in Fig. 1.3 (b), the thin film which is exposed to ambience other than the contact area with LED package (TIM) would experience a higher temperature, because the substrate temperature will have higher value than ambience, so there will be an increase in heat transfer area than the conventional TIM area. Thus, using solid thin film TIM cum heat spreader adds more efficient rate of heat transfer through convective and conductive modes which is impossible with conventional TIM pad.

Thermo imaging camera would be used in this research to explore and illustrates the mode of heat transfer through the samples under study and show the significance of the thin film coating extension (heat spreading and transfer in the in-plane direction) towards decreasing the LEDs surface temperature.

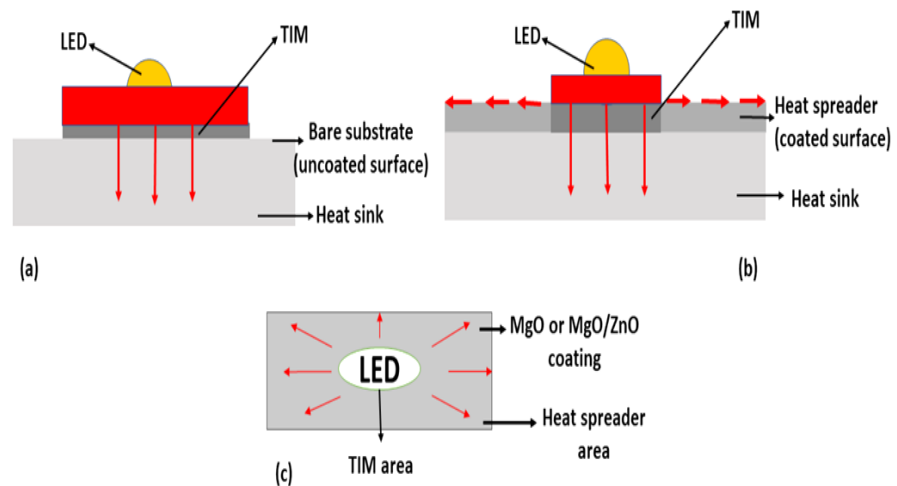


Figure 1.3 Illustration of LED mounted on TIM and showing heat dissipation via (a) the TIM only, (b) the TIM and through the in-plane direction (coated and exposed area to the ambient), (c) top view of Fig. 1.3 (b)

## 1.7 Research Novelty

A lot of projects have been carried out on the usage of MgO as conductive filler in the polymer matrix and fabricated MgO nanoparticle filled epoxy composites as heat transfer or TIM in the thermal management application. Since MgO has excellent thermal and structural behaviors, there is no report available on utilizing monolithic MgO or multilayer MgO/ZnO composite solid thin film as TIM or heat spreader on Al or Cu substrates for efficient thermal management in LED packaging. Therefore, this research project is undertaken to synthesis, optimize, investigate, and explore monolithic MgO and multilayer MgO/ZnO composites solid thin film TIM cum heat spreader the prepared MgO and MgO/ZnO multilayer are used as TIM cum heat spreader and to be tested on changing/improving the thermal and optical performance of high-power LEDs.

## 1.8 Thesis Outline

**Chapter 1- Introduction:** This chapter highlights the introduction of light emitting diodes, challenges faced by the lighting industries, problem statement and the purpose of the present study.

**Chapter 2 – Literature review:** This chapter discusses the literature and valuable novelties by other researchers regarding the LEDs' thermal management, reviews on MgO and ZnO thin film deposition techniques. Reviews on commercial TIM with their reliability and drawbacks are also discussed.

**Chapter 3 – Methodology:** This chapter explains in detail the methodology employed in preparing the substrates, synthesis of the thin films, characterization and analysis performed on the coated substrates.

**Chapter 4 – Results and Discussion Monolithic MgO Thin Film:** This chapter emphasizes the results and data together with their corresponding discussion from the analysis and characterization performed on monolithic MgO thin films.

**Chapter 5- Results and Discussion Multilayer MgO/ZnO Thin Film:** This chapter emphasizes on comparative studies and discussion from the analysis and characterization performed on monolithic MgO and multilayer MgO/ZnO thin films. Thermal, optical, and IR imaging performance of LEDs mounted on MgO/ZnO heat spreader are also explained and presented in this chapter.

**Chapter 6 – Conclusion and Recommendation:** This chapter recaptures the main objectives of the research work, the summary and conclusion of the research work in this project. Future suggestion and recommendation to improve MgO thin film heat spreader are also part of this chapter.

## **CHAPTER 2**

### **LITERATURE REVIEW**

#### **2.1 Overview**

A lot of research work have been performed to address thermal management challenges in LEDs and come up with possibilities for enhancing heat dissipation techniques from the LED's package. This chapter focuses on literature reported by many researchers on the fundamentals of heat transfer and concepts of heat dissipation in LEDs. The importance of TIM, solid thin film TIM or heat spreader and literature on techniques employed in the deposition of solid thin films have been explored in this chapter. Similarly, this chapter highlighted LEDs thermal and optical performance evaluated by thermal transient characterization using different types of TIM and heat spreaders.

#### **2.2 Thermal management of LEDs**

Continuous advancement in LEDs miniaturization, lifespan, efficient thermal performance, environments adaptation, targeted reduction in purchasing cost and improvement in converting the input energy into the light are being attained by the lighting technology industries [29, 30]. Recently, CREE lighting industry using AlGaN technology attained 30-40% efficiency level with green lighting devices and 50-60% efficiency from blue and UV devices, they moved ahead to achieve an efficient and energy-saving white light source from appropriate combinations of red, green and blue LEDs. The second approach uses a combination of blue or UV LEDs and a phosphor to achieve a white light source [29]. Despite those achievements attained by the lighting technology industries, many generated photons are confined within the LEDs

package due to miniaturization and inefficiency of semiconductors that produce the light [30 -32]. Evidence had proven that only 20-30% of critical heat generated within the package are dissipated to outside the device; this limit further development of highly efficient working LEDs [25, 26, 30]. This critical heat if not dissipated to the ambient properly, will cause a rise in the junction temperature of the LEDs, shifts in output wavelength, yellowing of the white light, decrease in forwarding voltage, mechanical failure, and deterioration in the overall efficiency of the LEDs [33 - 35]. Therefore, a proper heat transfer path is required for removing the heat to the environment without altering the reliability of the devices.

Advanced research is focused on adopting proper thermal management to achieve reliability and optimum thermal as well as the optical performance of LEDs. The researchers aimed at improving both internal and external thermal management of LEDs. Internal thermal management involves the mechanism of transfer of heat from the p-n junction to the LED substrate. In contrast, external thermal management is the dissipation of the heat from the substrate to the surrounding environment [36 – 38]. Figure 2.1 described the process involved in heat dissipation from the LEDs to the environment. Internal thermal management can be related to heat transfer through conduction mechanism; therefore, this process requires a substrate material with high thermal conductivity such as PCBs, MCPCBs, aluminum and copper [39, 40].

The external thermal management involves conduction, convection and radiation mechanism, and the conduction heat transfer process involves molecular excitement within the materials in contact without bulk motion of their matter.

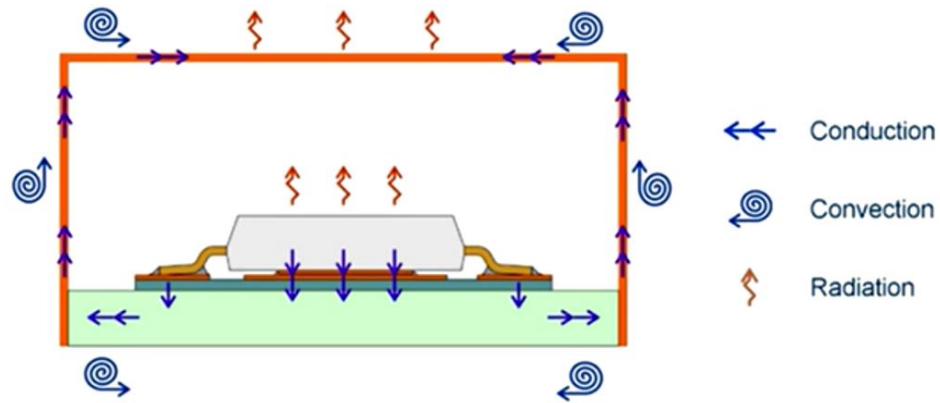


Figure 2.1 Heat transfer via conduction, convection, and radiation from the LED to the environment [38]

While the convection process requires passing the heat energy across the cold heat sink surface and employ a thermal diffusion process to remove the heat energy from the hotter body into the ambient. The radiation aspects solely depend on the LED's temperature and surface area. To maintain the temperature of LEDs, the heat generated at the junction, especially high-power LED would be entirely removed to the ambient by suitable heat transfer path [33]. Solid state lighting industries continue to develop numerous LEDs thermal management technologies which include active solutions, passive solutions, PCBs, and TIM. Active cooling technology requires forced conventional motorized fans.

In contrast, passive cooling technology operates under the influence of metal heat-sinks, ice heat-sink or heat pipes to extract heat out from LEDs [33]. Active and passive cooling technology are not suitable for LEDs that should be in an enclosed area or hot climates rather PCBs or TIM is preferable. The PCBs, MCPCBs or TIM is sandwiched between the LEDs package and heat sink to expedite heat transfer to the ambient efficiently. Figure 2.2 illustrates how heat is transferred from the LED through the MCPCBs, TIM, heat sink to the ambient.

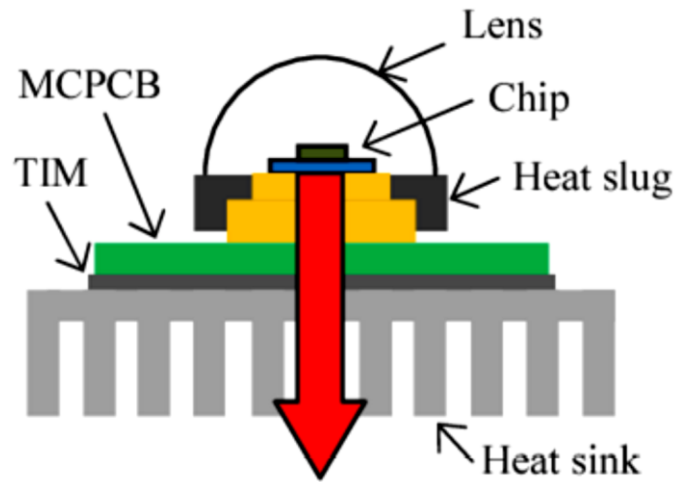


Figure 2.2 Schematic diagram of heat transfer mechanism from LED package to the ambient [41]

Continuous research was done to improve the heat transfer path efficiently, even in very low driven currents. Approaches of improving the thermal conductivity of the thermal path were accomplished by using thermally conductive ceramic materials as substrates such as BN, AlN, Al<sub>2</sub>O<sub>3</sub> and so on as an alternative dielectric layer material in PCB or MCPCBs. The thickness of the dielectric layers was reduced to optimum together with improvement in the quality of their interface [39]. Similarly, in an effort of enhancing the heat transfer capacity of the substrates, TIMs were introduced or coated over the substrates [39, 42 -44]. The advanced substrates were expected to increase heat transfer coefficient from the LEDs package, lower the junction temperature and thermal resistance of the device, and finally improve the thermal and optical output of LEDs [6, 7]. Thus, improvement in the heat transfer path is essential for effective and reliable thermal management.

### **2.3 Significance of thermal management in electronic and optoelectronic devices**

As electronics and optoelectronic components continue to undergo further miniaturization, so do more and more heat is generated within the components. In consequence, there is an urgent requirement to dissipate the critical heat from hot chips to the ambient effectively to ensure low thermal resistance, lifetime, and mission of the packages. Propose solution should possess some qualities such as high thermal conductivity, good mechanical properties, thermally and chemically stable, low coefficient of thermal expansion, cost-effective, environmentally friendly, fast to develop and easy use [45, 46]. The heat sink was earlier fixed to the heat source for heat dissipation; however, they have restricted size issues for miniaturization package shape and prone to thermal cracking [47]. Therefore, varieties of alternative thermal management approaches emerged. This involved designing and sandwiching thermal interface material between the heat source and a heat sink. The TIMs furnish heat conduction across the mating surfaces and enhance the thermal performance addition to the reliability of the electronic or lighting device. Generally, TIMs are polymer-based composites. The thermally conductive fillers are loaded into the polymer matrix and mixed thoroughly to obtain uniform composite. The fillers include silver, copper, BN, AlN, SiC, MgO, Al<sub>2</sub>O<sub>3</sub> or ZnO. Under the influence of average pressure, the TIMs are recommended to filled voids created by non-smooth mating surfaces and replaces the air gaps that exist within the void with the conductive fillers, and this improves heat conduction through the solid TIMs (Figure 2.3) [12]. Considering those requirements and reasons, TIMs from polymer composites are being designed and developed rapidly for thermal management purpose.

## 2.4 Heat transfer through thermal interface materials

Thermal interface material is usually sandwiched between two mating solid surfaces (LED package and heat-sink) to overcome the imperfection that exists between the surfaces and increasing heat transfer coefficient. TIM are thermally conductive materials that are used to treat surfaces deficiencies, roughness and fill up the multiples air voids between the two solid surfaces and thus, improve the thermal conductivity of the path and reduces their thermal resistance [48]. Figure 2.3 illustrates the capability of TIM in filling the micro and macroscopic air voids cause from the two mating solid surfaces. Since TIMs are more thermally conductive than air, their presence would improve the thermal contact between the two interfaces and increase the rate of heat dissipation from the LEDs to the heat-sink.

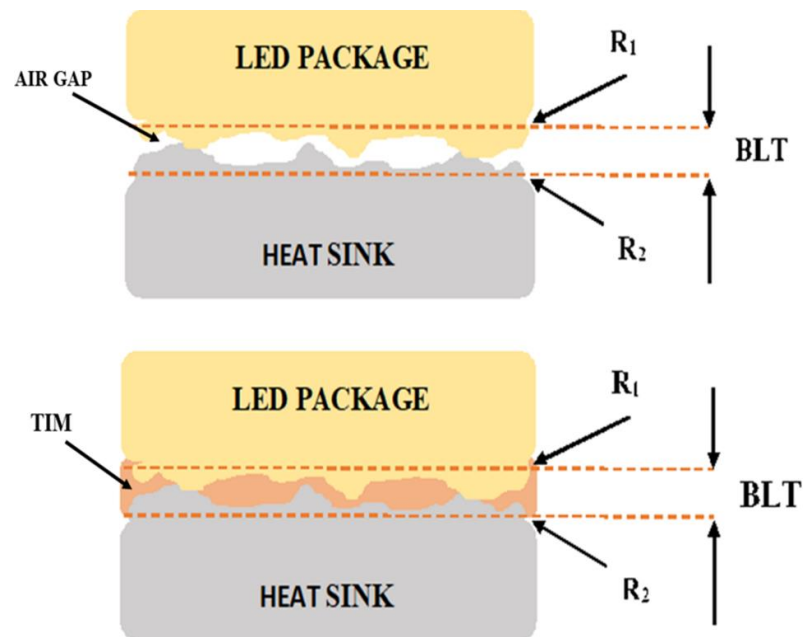


Figure 2.3 Schematic illustration of TIM filling in the air gap between LED package and heat sink

For any material to be suitable as an interface medium, the material is expected to possess high thermal conductivity than air, low coefficient of thermal expansion and provision of low thermal contact resistance. Wonjun et al. [49] developed a reliable few-layer graphene composite thermal interface materials, and they reported that selection of a high conducting material made them achieve low contact resistance of 3.2 mm<sup>2</sup>K/W and enhancement in thermal conductivity of the graphene composite TIM. Filling the air voids with high thermally conductive nitrides, carbides or metal oxides will raise the conductivity of the interfaces, speed up in heat dissipation and subsequent reduction in both junction temperature and thermal resistance of LEDs under test. Advancement was also made in eliminating minor surface defects that exist between PCBs and heat sink by the introduction of TIM between them, thereby improving the thermal path conductivity [41 – 44].

In addition to thermal path thermal conductivity improvement, reduction in thermal contact resistance between two solid objects in contact and increase in heat conduction, the TIM introduced must possess a reasonable thickness that can conform to the interface mission, displacement of multiple voids, ensured minimized total thermal resistance and longtime thermal stability. To achieve a minimum total thermal resistance ( $R_{th-tot}$ ), individual thermal interface resistance across the junction of the three materials in contact must be considered as illustrated in Figure 2.4 and there should be a uniform heat transfer across the TIM [27, 50]. The significant total thermal resistance at interface between the LED package and the heat sink is the sum of the resistance due to the TIM's thermal conductivity and contact resistance between the TIM and LED package surfaces and the heat sink surface. Equations 2.1 and 2.2 gives the total thermal resistance across the interfaces of three materials in mutual contact,

$$R_{th} = R_{LED/TIM} + R_{TIM} + R_{TIM/Heat-sink} \quad (2.1)$$

$$R_{th} = R_{LED} + \frac{BLT(t)}{K_{TIM}} + R_{Heat-sink} \quad (2.2)$$

Where  $R_{LED/TIM}$  is the contact resistance between LED and TIM,

$R_{TIM} = \frac{BLT(t)}{K_{TIM}}$  is the resistance due to thermal conductivity of the TIM,  $BLT(t)$

is the thickness of the TIM,  $K_{TIM}$  is the thermal conductivity of the TIM, and  $R_{TIM/Heat-sink}$  is the contact resistance between TIM and heat-sink.

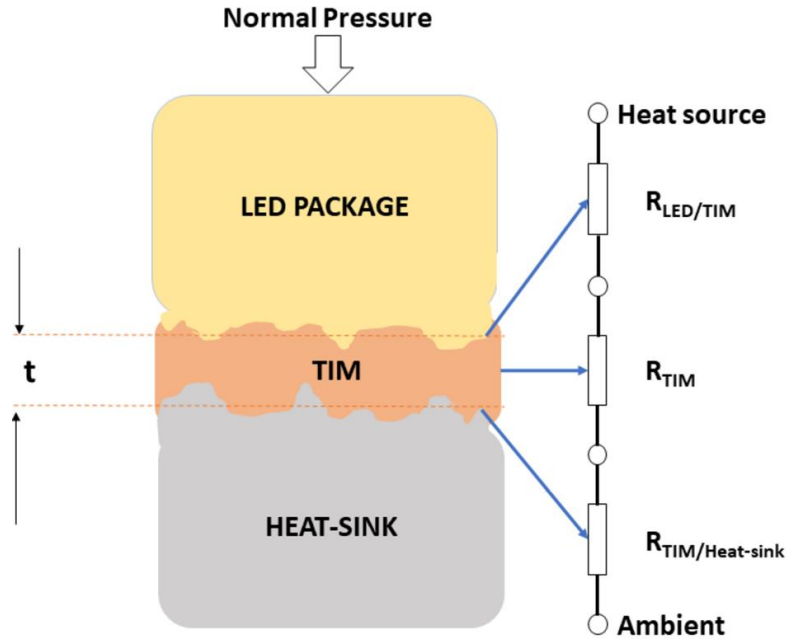


Figure 2.4 Model diagram for contact thermal resistance for LED, TIM and heat-sink set up

TIMs helps in unifying the heat flow direction as well as heat conduction enhancement from LED and electronics packages to the ambient, an overall decrease in the device's junction temperature together with thermal resistance.

There are varieties of commercially available TIM; they include thermal putties, grease, paste, phase change materials, gels, thermally conductive adhesives, elastomeric pads, and epoxies compound [50 – 61]. TIMs fabrication processes involved dispersing high thermally conductive particles (fillers) such as Al, Ag, Cu, BN, AlN, MgO, Al<sub>2</sub>O<sub>3</sub> or ZnO within a polymer matrix or silicone grease [13, 27, 53].

The aim is to improve the thermal conductivity and mechanical properties of the polymer matrix.  $\text{Al}_2\text{O}_3$  and  $\text{ZnO}$  ceramic fillers dispersed in silicone rubber and used as the thermal pad was reported by Sim et al. [54]. Optimum thermal performance was recorded for  $\text{ZnO}$  filled silicone rubber thermal pad compared to  $\text{Al}_2\text{O}_3$  filled thermal pad; however, they proved restriction of the  $\text{ZnO}$  filled thermal pad TIM to power devices to avoid drastic degradation of the device components [54]. Zeng et al. in their research attained both high thermal conductivity (1.46 W/mK) and phase enthalpy change (76.5 J/g) improvements for Ag filler dispersed in organic phase change material (PCM) TIM [55]. In conforming to the relationship between the electronics package and heat-sink, Chia-pin et al. sandwiched thermal grease TIM between the mating surfaces [56]. An improved interface void reduction, high interface thermal conductivity, low thermal contact resistance and efficient device thermal performance were recorded with thermal grease TIM of low thickness. It was observed that total interface resistance and surfaces voids increased with a thermal grease TIM of high thickness. In a separate study, highly thermally conductive metal, and ceramic fillers of Al and AlN were integrated with epoxy resin respectively by Anithambigai et al. for effective LED thermal management [57]. Results from the study indicated enhancement in heat dissipation from 3 W LED mounted on the epoxy resin composite TIM and subsequent reduction in both junction temperature and total thermal resistance of the LED. Dianyu et al. [58] carried out work on silicon carbide nanowires (SiC NWs) and silicon carbide micron particles (SiC MPs) fillers filled epoxy resin. It was observed with 3.0 wt% filler the thermal conductivity of SiC NWs/epoxy composites reached 0.449 W/mK improvement compared to 0.329 W/mK and 0.10 W/mK for SiC MPs/epoxy composites and neat epoxy, respectively. John et al. [59] recorded 4.0 W/mK thermal conductivity achievement with 42 vol% of BN filled

epoxy-thiol system. Improvement recorded in the heat transfer rate in this research is correlated to the intrinsic thermal conductivity and volume of BN particles dispersed in the system. Extensive research to generate new and improves the properties of graphene-epoxy nanocomposites for electronic packaging and insulation application was reported by Fei-peng et al. [60]. Results from the research showed MgO filler dispersed into graphene-epoxy composite not only improved the interfacial bonding between the graphene and the epoxy but enhanced the thermal conductivity of the epoxy from 0.2210 W/mK to 0.3819 W/mK while preserving the entire electrical insulation of the composites. The prepared MgO/graphene/epoxy nanocomposites exhibited significant thermal conductivity and electrical insulation that would make the composites a good prospect for thermal management. Nakagawa et al. worked on MgO particles filled epoxy resin for heat-dissipating grease, the heat-dissipating coating and TIMs for electronics and lighting packaging system. The size of the MgO particles plays a role in suitability of the filler in shaping the thermal conductivity, heat resistance and electrical insulation of the composites [61]. The use of MgO filler in an epoxy molding compound (EMC) was reported by Andrew et al. stating that MgO is inexpensive, electrically insulative, nontoxic and has high intrinsic thermal conductivity for optimum thermal transfer attainment [14]. Thermal conductivity of 3.0 W/mK was successfully achieved with 56 vol% of MgO filler introduced into the epoxy molding compound. Results from related literature showed the significance of MgO fillers by improving more in the thermal conductivity of the polymer composites compared to other fillers. Thermal conductivity of 3.0 W/mK was recorded for 56 vol% of MgO dispersed into epoxy resin compared to 1.68 W/mK, 0.74 W/mK, 1.11 W/mK, 0.59 W/mK, 0.57 W/mK, and 0.81 W/mK recorded for 44.3% graphene, 68.25% Cu, 69.69% Al, 35.5% BN, 67% Al<sub>2</sub>O<sub>3</sub>, and 66.3% ZnO powders dispersed in

epoxy, respectively. The MgO/epoxy composite thermal conductivity appeared to be higher also than 0.346 W/mK recorded for 2.5% SiC/SiO<sub>2</sub> nanowires dispersed in epoxy resin [14, 62, 63]. The MgO fillers happened to be inexpensive and nontoxic compared to BeO, BN, and AlN though those fillers possessing higher bulk thermal conductivity. Despite remarkable achievements recorded by the epoxy composites, the effective thermal conductivity of the composites TIMs are within the range of 5-10 W/mK, which is lower than the individual thermal conductivity of the two mating solid objects [27]. Also, thermal paste experiences squeezing and phase segregation, causing the paste not to be thermally stable all the time [64]. Apart from low thermal conductivity and lack of thermal stability; the polymer-composites TIMs suffers from high *BLT*, air void within them, porous structure, pumped out, mechanical stress and cracks during thermal expansion and contractions of the mating objects as well as the requirement of limited pressure to establishes mutual contact between the mating surfaces and the TIMs so that heat can flow uniformly and perfectly [64 – 66]]. Consequently, shortcomings experienced from polymer composites TIMs caused a rise in  $T_j$ ,  $R_{th}$  and the severe failure of the entire devices. Solid thin films TIMs have been used as an alternative to the polymer based TIMs due to provision of high composite thermal conductivity above 10 W/mK, good adhesion to various metal substrates; and the thickness of the thin film can be controlled by either increasing or minimizing the layers of the coating. Such features can help improves the heat transfer rate and thermal performance of devices.

#### **2.4.1 Significance of Thin Film Solid Materials as TIM**

Solid thin film is suggested as an alternative TIM towards overcome challenges such as low thermal conductivity, degradation when exposure to high temperature,

poor resistance to organic solvents, dry out and pop out faced by polymer composites TIMs. Therefore, thermally conductive ceramics (BN, AlN, MgO, Al<sub>2</sub>O<sub>3</sub> or ZnO) or metals (diamond, Ag, Cu, or Al) would be deposited over metal (Al or Cu) substrates as thin films TIMs, doing so would result to attainment of composites materials with thermal conductivity higher than those of polymer composites TIMs. The solid thin film TIMs also have the capability to possess some properties such as (low surface roughness, optimum *BLT*, resistance to organic solvent and capable of withstanding high temperature without degradation) better than those of polymer composites TIMs. Those qualities of solid thin film TIMs will ensure mutual contact, eliminate air voids between the contacting bodies and provide effective heat transfer path.

#### **2.4.2 Heat Transfer through Solid Thin Film Thermal Interface Materials**

The benefits of using thin film base TIMs for LEDs thermal management were several pieces of literature unveiled a significant upgrade in thermal performance. Lim et al. proved the reliability of RF sputtered Cu-Al<sub>2</sub>O<sub>3</sub> thin film TIM for efficient LED thermal management. They recorded thermal resistance difference ( $\Delta R_{th}$ ) of 5.28 K/W and lower junction temperature difference ( $\Delta T_j$ ) of 12.3 °C for 3 W LED mounted on the Cu-Al<sub>2</sub>O<sub>3</sub> compared to values recorded for LED fixed to bare Al substrate [44]. To improve heat dissipation, improve output performance and reliability of LEDs, Shanmugan et al. deposited Al<sub>2</sub>O<sub>3</sub> on Cu substrate and used it as TIM. Finding from their research is presented in Table 2.1. Comprehensive results in Table 2.1 highlighted LED attached to non-annealed 400 nm/Al<sub>2</sub>O<sub>3</sub> thin film obtain low  $R_{th}$  (46.72 K/W) and low  $T_j$  (52.24 °C) values compared to other boundary conditions [67]. Mutharasu et al. conducted a research work on designing and fabricating ZnO thin film TIM for LED thermal management. High differences in junction temperature (6.35 °C) and

total interface resistance (2.41 K/W) were recorded for high-power LED mounted on 200 nm thickness of ZnO thin film TIM when compared with bare Cu substrate at 700 mA [68]. In a similar work, Shanmugan et al. deposited BN thin film over Al substrate and used as a heat sink. Thermal performance of LEDs mounted on BN thin film TIM, commercial thermal paste, and bare Al substrate were evaluated. Results from the analysis indicated LED mounted on BN thin film TIM displayed higher differences of ( $\Delta T_J = 2.97 \text{ }^\circ\text{C}$ ), and ( $\Delta R_{th} = 1.92 \text{ K/W}$ ) with a noticeable increment on luminosity at 700 mA respectively [69]. To test the capability of thin film TIM for LEDs packaging, Mah et al. used a co-precipitation technique to deposit Ag-ZnO thick film on Al substrate. They achieved  $R_{th}$  of 13.81 K/W and  $T_J$  of 47.32  $^\circ\text{C}$  at 500 mA for Ag-ZnO thick film with 7.0 wt% Ag dopant concentration, low surface roughness and minimum porosity within the film [70]. Shanmugan et al. used Chemical vapor deposition technique to synthesize  $\text{Al}_2\text{O}_3$  thin film on Al and used it as TIM for high power LEDs. Comparison between  $\text{Al}_2\text{O}_3$  thin film deposition time and annealing temperature showed how they influenced change in the films surface quality, low interface resistance and achievement of a high difference of rising in junction temperature ( $\Delta T_J = 4.34^\circ\text{C}$ ) [71].  $R_{th}$  and  $T_J$  extracted from the research is presented in Table 2.1. Shanmugan et al. [72] used RF sputtering to deposit ZnO thin film of different thickness on Al and used as TIM for high power LED. They recorded lowest surface roughness (5.3 nm), least peak-valley of 22-55 nm, the high difference in junction temperature ( $\Delta T_J = 7.46 \text{ }^\circ\text{C}$ ) and total thermal resistance ( $\Delta R_{th-tot} = 3.35 \text{ K/W}$ ) for ZnO thin film with 200 nm thickness. As expected, thin films with low surface roughness and least peak-valley to have efficient heat flow through them. Evidence gathered from the works of literature above proved suitability of thin film composites TIMs for efficient and reliable thermal management